

Transport Monte Carlo

Leo L. Duan*

Abstract: In Bayesian inference, transport map is a promising alternative to the canonical Markov chain Monte Carlo for posterior estimation: it uses optimization to find a deterministic map from an easy-to-sample reference distribution to the posterior. However, often the invertible map does not exist between the two distributions and can be difficult to parameterize with sufficient flexibility. Motivated to address these issues and substantially simplify its use, we propose *Transport Monte Carlo*. Instead of relying on a single deterministic map, we consider a coupling joint distribution modeled by a non-parametric mixture of several maps. Such a coupling is guaranteed to exist between the reference and posterior distributions. To automate the map parameterization and estimation, we use the invertible neural networks to replace the manual design procedure. Once the coupling is estimated, one can rapidly generate a large number of samples that are completely independent. With a carefully chosen reference distribution, the difference between the generated samples and the exact posterior is negligibly small. Both theoretic and empirical results demonstrate its advantages for solving common but challenging sampling problems.

1 Introduction

Bayesian paradigms have been routinely used for uncertainty quantification. Markov chain Monte Carlo, particularly the Gibbs sampling, has been the mainstream tool for the posterior estimation; updating via the conditional given the current state, a primary challenge is that the samples tend to be auto-correlated, leading low effective sample size. To be able to have a high accuracy estimate, one has to run a long simulation of the Markov chain. For a recent discussion on this issue, see Robert et al. (2018). A large literature of new Markov chain methods has been proposed, aiming to make each Markov state less dependent on the previous state. Methods include Metropolis-adjusted Langevin algorithm (Roberts et al., 1996), Hamiltonian Monte Carlo (Neal et al., 2011), piecewise deterministic (Bierkens et al., 2019), or continuous-time Markov chain Monte Carlo (Fearnhead et al., 2018). At the same time, there is some literature focusing on alternatives to Markov chain methods. For example, among others, Approximate Bayesian Computation (Beaumont et al. (2009)) avoids the evaluation of the likelihood and instead relies on a divergence between simulated and observed data in rejection sampling; variational Bayes (Blei et al., 2017) replaces the complicated posterior with the mean-field approximation that is easier to sample from. Despite the popularity, there are critical issues, such as ignoring the correlation among the parameters, and difficulty to quantify the approximation error for diagnostics. For the discussion and remedy on those issues, see Giordano et al. (2018).

Transport map is an interesting new solution (El Moselhy and Marzouk, 2012). To briefly review, let $\theta \in \Theta$ be a continuous parameter of interest, $\Pi_0(\theta)$ the prior probability density, Y the data and $L(Y; \theta)$ the likelihood. Slightly abusing notation, denote the random variable from the posterior as

$$\theta \sim \Pi(\theta | Y) = \frac{L(Y; \theta)\Pi_0(\theta)}{m(Y)},$$

where $m(Y) = \int L(Y; \theta)\Pi_0(\theta)d\theta$ is normalizing constant. Consider another random variable $\beta \in \mathcal{B}$ from another proper measure (with β having the same number of elements as θ), referred to as the reference distribution

$$\beta \sim \Pi_r(\beta).$$

*Department of Statistics, University of Florida, Gainesville, FL, email: li.duan@ufl.edu

If there exists an invertible map that pushes forward the reference measure to the posterior $f : \beta \rightarrow \Theta$. Using standard variable transformation $\theta = f(\beta)$, the pullback density from the posterior should equal to the reference one:

$$\frac{L\{Y; f(\beta)\}\Pi_0\{f(\beta)\}}{m(Y)}|\det\nabla f(\beta)| = \Pi_r(\beta), \quad (1)$$

with ∇f the Jacobian matrix. With f flexibly parameterized and satisfying invertibility, one minimizes the difference between the left (without the constant $m(Y)$) and right sides, using samples $\beta_i \sim \Pi_r(\beta)$. When the optimal is reached, $f(\beta_i)$ is the exact posterior sample, and they are completely independent — a major advantage compared to the Markov chain methods.

Despite its potentials, there are two limitations. First, most importantly, there is no guarantee that an invertible map exists between $\Pi_r(\beta)$ and $\Pi(\theta | Y)$. This is also known as the ill-posed Monge problem (Santambrogio, 2015). As an example, if $\Pi_r(\beta)$ is a bivariate Gaussian but $\Pi(\theta | Y)$ has one element fixed to a constant (Dirac measure), there is no map between the two due to the different dimensions. Even without the dimensionality issue, often f is parameterized with limited flexibility, which can lead to thinner distribution tails of $f(\beta)$, compared to $\Pi(\theta | Y)$. As shown in our later example, when $\Pi(\theta | Y)$ is multimodal, and the estimated $f(\beta)$ tends to converge to only one of the modes. As a remedy, existing methods instead use the transport to optimize Markov transition kernel from one state to the next (Parno and Marzouk, 2018). Despite some success, this arguably weakens the unique advantage of having independence in the samples. Second, the typical implementation relies on the manual design of f , as one has to choose a composite of several invertible functions. These procedures are cumbersome for the users. Recently some automated solutions have been proposed (such as Levy et al. (2018)), but to obtain samples $\theta_i = f(\beta_i)$, one needs to include every β_i in the optimization of f . This leads to poor scalability when the sample size is large. There is a clear but under-explored alternative: first estimating f on a smaller training set of β_i , then generating a large number of samples with f fixed. Empirically, the induced error is often negligible, although there has not been any theoretic justification to our best knowledge. Those strengths and weaknesses motivate us to propose a much more general and easier-to-use transport approach, that we call Transport Monte Carlo.

2 Method

2.1 Random Transport via Non-parametric Coupling

For a concise exposition, we focus on θ and β as continuous random variables. Extensions to other cases will be discussed at the end of the article. Consider a coupling, defined by the joint density P , between θ and β :

$$(\theta, \beta) \sim P(\theta, \beta),$$

$$\int P(\theta, \beta)d\beta = \Pi(\theta | Y), \quad (2)$$

$$\int P(\theta, \beta)d\theta = \Pi_r(\beta). \quad (3)$$

The coupling always exists — one trivial case would be the independent coupling $P(\theta, \beta) = \Pi_r(\beta)\Pi(\theta | Y)$. In fact, the transport map (1) is a special case of deterministic coupling $P(\theta, \beta) = \Pi(\theta | Y)\delta\{\beta - f^{-1}(\theta)\}$ (with δ the Dirac delta), which relies on a strong assumption that (2) and (3) can be met.

To relax this assumption, we instead consider a *random* transport, by modeling the conditional distribution of β given θ as a random choice of several invertible maps, parameterized by a mixture distribution

$$P(\theta, \beta) = P(\beta)P(\theta | \beta), \quad P(\theta) = \Pi(\theta | Y), \quad P(\beta | \theta) = \sum_{k=1}^K w_k(\theta)\delta\{\beta - f_k^{-1}(\theta)\}, \quad (4)$$

with the mixture weight $w_k(\theta) \geq 0$, $\sum_{k=1}^K w_k(\theta) = 1$ for any θ . We allow w to potentially change with θ for more flexibility (this includes the simpler case with w invariant to θ).

This mixture is inspired by the Bayesian non-parametric method to model an unknown conditional density (Dunson et al., 2007). The randomness in $P(\beta | \theta)$ has two benefits: (i) we relax the stringent equal dimensionality requirement, as $\Pi(\theta | Y)$ can have a lower measure dimension than $\Pi_r(\beta)$; (ii) we can now use simpler f with less worry on its flexibility, as it can be compensated with multiple f_k 's. The following theorem shows the existence of random transport as $K \rightarrow \infty$.

Theorem 1. *Under (4), assuming $\Pi_r(\beta)$ has an equal or higher dimension than $\Pi(\theta | Y)$, as $K \rightarrow \infty$ there exist $\{(w_k, f_k)\}_k$ such that (2) and (3) are satisfied almost everywhere.*

Under this generalization, the random transport still enjoys an equality connecting $\Pi_r(\beta)$ and $\Pi(\theta | Y)$, after marginalizing over k .

Theorem 2. *Under (3) and (4),*

$$\Pi_r(\beta) = \sum_{k=1}^K w_k \{f_k(\beta)\} \Pi\{f_k(\beta) | Y\} |\det \nabla f_k(\beta)|. \quad (5)$$

2.2 Transport Monte Carlo

With the above results, we can now develop a Transport Monte Carlo algorithm, which consists of two stages: (i) optimizing f and w using a set of training samples $\beta_1, \dots, \beta_n \sim \Pi_r$; (ii) generating new samples θ using the estimated f and w . In the first stage, we minimize

$$Loss = \frac{1}{n} \sum_{i=1}^n \log g(\beta_i), \quad g(\beta_i) = \frac{\Pi_r(\beta_i)}{\sum_{k=1}^K w_k \{f_k(\beta_i)\} L\{Y | f_k(\beta_i)\} \Pi_0\{f_k(\beta_i)\} |\det \nabla f_k(\beta_i)|}, \quad (6)$$

which is related to the empirical Kullback-Leibler divergence as $Loss + \log m(Y)$.

After the optimization converges, in the second stage, we sample new β and θ via

$$\begin{aligned} \beta &\sim \Pi_r, \\ \theta &\sim \text{Categorical}(v_1, \dots, v_K), \\ v_k &\propto w_k \{f_k(\beta)\} \Pi\{f_k(\beta) | Y\} |\det \nabla f_k(\beta)|. \end{aligned} \quad (7)$$

We separate these two stages because the optimization is the time-consuming step, using a smaller set of samples reduces the computing cost; while the sampling is embarrassingly parallel and we can rapidly obtain a large number of samples.

2.3 Automated Computation for Invertible Maps

A major complexity of the transport-related methods is in parameterizing and estimating the invertible maps. To simplify and automate this process, we exploit the popularity of neural networks and their computational toolbox.

Following Dinh et al. (2017), we parameterize each f_k as an M-layer invertible neural network. Without loss of generality, assuming β is a p -element vector. We set each layer as a p -element to p -element transform:

$$\begin{aligned} f_k(\beta) &= \sigma_1^k \circ \sigma_2^k \circ \dots \circ \sigma_M^k(\beta) \\ \sigma_m^k(x) &= [x_A * s_A^k(x_B) + t_A^k(x_B), x_B]' \text{ if } m \text{ is even} \\ \sigma_m^k(x) &= [x_A, x_B * s_B^k(x_A) + t_B^k(x_A)]' \text{ if } m \text{ is odd} \end{aligned} \quad (8)$$

where $*$ denotes the Hadamard product; $\{A, B\}$ are the partition of the indices; s_A, s_B, t_A and t_B are nested neural networks with a flexible forms (not necessarily invertible), with the only requirement that $s(x) > 0$.

Each σ_m^k resembles a location-scale transform, except the magnitudes of scaling and shifting also depend on the input, making the change non-linear. Although the nested s , and t , have flexible forms, the enclosing σ_m is invertible $\sigma_m^{-1}(x) = [\{x_A - t_A(x_B)\}/s_A(x_B), x_B]'$ for even m , $\sigma_m^{-1}(x) = [x_A, \{x_B - t_B^k(x_A)\}/s_B^k(x_A)]'$ for odd m . Therefore, the whole f_k is invertible. In addition, $\det \nabla f_k(\beta) = \prod_{\text{all } s^k} s_{:,l}^k$, with $s_{:,l}^k$ the output elements of s_A^k and s_B^k in the neural network $f_k(\beta)$. See Dinh et al. (2017) for the detailed derivation. For $w(\theta)$, we parameterize it similarly to f_k except using an extra layer of Softmax activation, so that the output is in Δ^{K-1} . We parametrize s , and t , with a simple neural network with one hidden layer, connected by the leaky ReLU activation function; the last layer of s is exponentiated so that each element is positive; we use $M = 5$ in all the examples. Compared to a manually designed f , the neural network is much more flexible. In addition, it allows us to exploit popular computing toolbox such as PyTorch (Paszke et al., 2017), making it easy to implement. The optimization utilizes stochastic gradient descent, by randomly generating a new batch of β_i 's in each iteration for gradient calculation. In this article, we use a batch size of 1,000 and run over 1,000 iterations, yielding $n \geq 10^6$. For tractable computation, we approximate infinite K with a truncated $K = 20$ in most examples, and found empirically no difference compared to using larger K .

2.4 Generalization Error and Choosing the Reference Distribution

As described above, the samples of (β, θ) are generated using f and w , estimated from a finite training set of β_i 's. There can be a small difference between the sampled distribution and the exact posterior, which we will refer to as the generalization error (based on some resemblance to the common training-and-prediction task). Such an error can be quantified theoretically, providing a guide on choosing the reference Π_r . To distinguish from the training samples, we will use β^* and θ^* instead to denote the newly generated samples.

Note that each training sample β_i has a common minimized value $g(\beta_i) = -\log m(Y)$, when (5) holds. Intuitively, when β_i 's are dense enough to cover most of the region in $\Pi_r(\beta)$, the new sample β^* will be near a certain β_i 's with high probability, hence the associated loss $g(\beta^*)$ should be near the minimized loss as well. This concept can be formalized as a high probability ϵ -net, defined as

$$\beta_{\epsilon, \delta} = \left\{ (\beta_1, \dots, \beta_n) : \int_{\mathcal{A}} \Pi_r(\beta) d\beta \geq 1 - \delta, \mathcal{A} = \left\{ \beta \in \beta : \inf_{i \in \{1 \dots n\}} \|\beta - \beta_i\| \leq \epsilon \right\} \right\}.$$

We now formally state the conditions.

Theorem 3. *Suppose the training samples $(\beta_1, \dots, \beta_n) \in \beta_{\epsilon, \delta}$, and further if*

1. $\Pi(\theta | Y)$ and $\Pi_r(\beta)$ are absolutely continuous with respect to Lebesgue measure,
2. each s in (8) is Lipschitz continuous and bounded,

then

$$\inf_{i \in \{1 \dots n\}} \|\log\{g(\beta^*)\} - \log\{g(\beta_i)\}\| = \mathcal{O}(\epsilon),$$

with probability $1 - \delta$.

Practically, this theorem relies on a high probability ϵ -net achieving small ϵ under moderate size n . Therefore, an important task is to choose a good Π_r with ϵ decreases rapidly in n . This is associated with the classical problem of bounding maximal spacing as the sample size increases (Janson, 1987). The multivariate normal, commonly used in transport-related methods, is in fact sub-optimal for this purpose as $\epsilon \approx O(p/\sqrt{\log n})$ (Deheuvels et al., 1986). Instead, in this article we choose uniform distribution $\Pi_r(\beta) = \text{Uniform}(0, 1)^p$, which has a much faster rate $\epsilon \approx O\{(p \log n)/n\}$ (Devroye et al., 1982). For a more involved but tighter bound, see Janson (1987).

For diagnosis, we have an error estimator using the empirical Kullback-Leibler divergence

$$KL\{\Pi(\theta^*) \|\Pi(\theta | Y)\} = \frac{1}{n^*} \sum_{i=1}^{n^*} g(\beta_i^*) + \log m(Y).$$

For intractable $m(Y)$ is, we replace it with a plug-in estimator $\widehat{\log m} = -(1/n) \sum_i \log g(\beta_i)$.

3 Numeric Illustrations

3.1 Multi-modal Posterior

We first sample from the posterior from a multivariate Gaussian mixture. Consider a posterior from the two-component mixture with unequal component means and unequal covariances

$$\Pi(\theta | Y) = 0.5\text{No}\left(\theta; \begin{bmatrix} 1 \\ 2 \end{bmatrix}, \begin{bmatrix} 1 & 0.5 \\ 0.5 & 1 \end{bmatrix}\right) + 0.5\text{No}\left(\theta; \begin{bmatrix} 6 \\ 2 \end{bmatrix}, \begin{bmatrix} 1 & -0.9 \\ -0.9 & 1 \end{bmatrix}\right).$$

We choose this example for two reasons: (i) to demonstrate the deterministic transport map can fail even in some simple cases, and how multiple maps in Transport Monte Carlo can solve this issue; (ii) we leave out the normalizing constant $m(Y) = 2\pi$ when implementing the loss function (6), and test the accuracy of the plug-in estimator $\widehat{\log m}$.

As shown in Figure 1(b), the deterministic transport map fails to discover the second component, even though the two means are not too far apart. This is due to the different covariances, particularly the different correlation signs, creating difficulty for one transport map to adequately accommodate two parts (we additionally verify that it does not have this issue when the covariances are equal). On the other hand, as shown in Figure 1(c), Transport Monte Carlo correctly identifies both modes as it exploits multiple transport maps. The estimated $\widehat{\log m} = 1.830$ (based on $n = 1,000$ training samples), is very close to the true $\log m(Y) \approx 1.837$. To assess the new sample error, we generate another 10,000 samples, and the empirical Kullback-Leibler divergence is only 0.011. As a comparison baseline, the kernel-based Kullback-Leibler estimates (Boltz et al., 2009) between the two exact samples from $\Pi(\theta | Y)$ is 0.009 ± 0.004 . This suggests that the Transport Monte Carlo sampler has high accuracy.

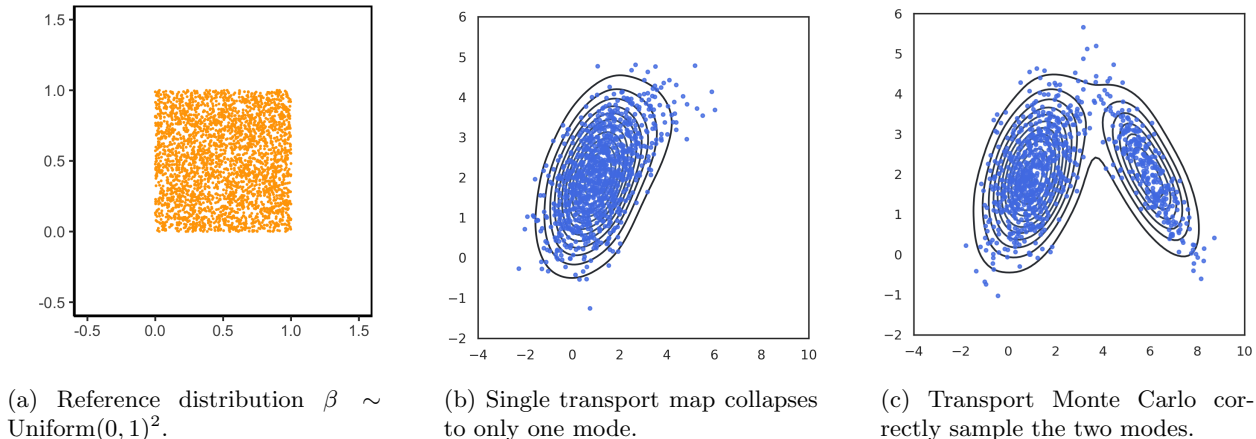


Figure 1: Comparing the performance of transporting from a uniform distribution (panel a) to bi-modal distributions. Transport map, with a single deterministic invertible map, fails to discover the second mode (panel b), while Transport Monte Carlo correctly estimates the posterior.

3.2 High-Dimensional Parameter

To illustrate the performance with the high dimensional parameter, we consider a sparse linear regression with the regularized horseshoe prior (Piironen and Vehtari, 2017). For data index $j = 1, \dots, N$ and covariate

index $k = 1, \dots, p$,

$$\begin{aligned}
 y_j &\sim \text{No}(x_j' b, \sigma_0^2), \\
 b_k &\sim \text{No}(0, \tilde{\lambda}_k^2 \tau^2), \quad \tilde{\lambda}_k^2 = \frac{c^2 \lambda_k^2}{c^2 + \tau^2 \lambda_k^2}, \quad \lambda_k \sim \text{C}^+(0, 1), \\
 c^2 &\sim \text{Ga}^{-1}(v/2, vs^2/2).
 \end{aligned}$$

where $x_j \in \mathbb{R}^p$ is the covariate; C^+ denotes the half-Cauchy and Ga^{-1} the inverse-gamma. Compared to the original horseshoe (Carvalho et al., 2010), the large signals are approximately subject to normal prior $\text{No}(0, c^2)$, instead of Cauchy, hence has a finite prior mean. However, due to the modification, Gibbs sampling is no longer applicable and the Hamiltonian Monte Carlo is suggested.

When simulating the data, we use $p = 2,000$ and $N = 100$; $\sigma^2 = 0.01$; $x_{j,k} \stackrel{iid}{\sim} \text{No}(0, 1)$; $b_k \sim \text{No}(5, 1)$ for $k = 1 \dots 5$, and $b_k = 0$ for $k = 6 \dots 2000$. For both σ^2 and τ^2 , we use the informative prior $\text{Exp}(100)$ to induce low noise and shrinkage global scale; for c^2 , we set $v = 5$, $s = 10$, as suggested by Piironen and Vehtari (2017). The results are compared with Hamiltonian Monte Carlo, using the No-U-TURN sampler provided by the PyMC3 package. As most of the parameters are close to the degenerate zero, Hamiltonian Monte Carlo can only use small leap-frog step, resulting in extremely slow mixing (2). We run it for 100,000 iterations and thin the chain at every 100 steps, and use them as the posterior sample. This takes approximately 8 hours. In contrast, the Transport Monte Carlo only takes a few minutes in optimization and can generate new samples almost instantaneously. Due to independence, no thinning is needed. The results are almost identical to the one obtained in costly Hamiltonian Monte Carlo.

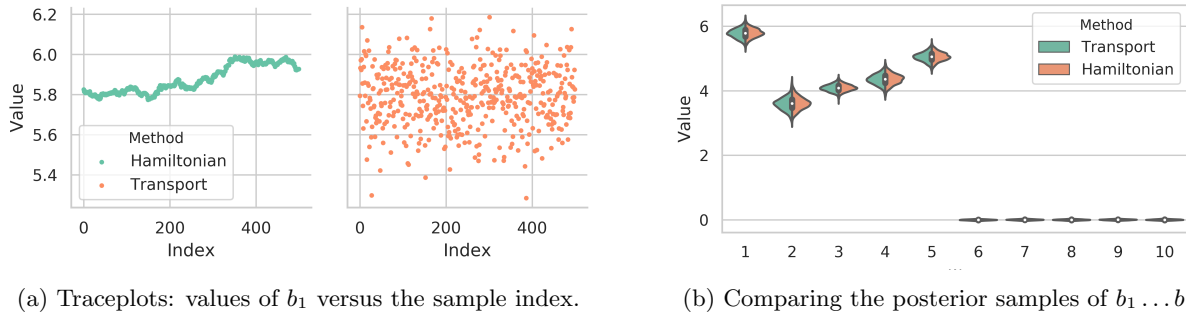


Figure 2: Comparing the performance of Hamiltonian Monte Carlo and Transport Monte Carlo in high dimensional sparse regression. The samples collected from Hamiltonian Monte Carlo are highly correlated (panel a, left), due to the small step size forced by most of b_k being close to zero; while the ones from Transport Monte Carlo are completely independent (panel a, right). The collected posterior are almost indistinguishable, despite the dramatic difference in computing efficiency (panel b).

4 Discussion

We show that Transport Monte Carlo can serve as an appealing alternative to conventional Markov chain Monte Carlo methods, and enjoys theoretic justification via coupling. On the other hand, several limitations remain and merit future work. Unlike Markov chain Monte Carlo, there is no asymptotic exactness guarantee as the number of samples goes to infinity. A possible correction amenable to the high dimensional parameter is using the obtained sample as initial values to start parallel Markov chains (Hoffman et al arXiv preprint-1903.03704). Another extension is to consider θ in a discrete or constrained space. There has been some solution proposed for discrete transport (Tran et al., 2019), nevertheless, a careful measure-theoretic study is still an interesting open problem.

References

- Beaumont, M. A., J.-M. Cornuet, J.-M. Marin, and C. P. Robert (2009). Adaptive Approximate Bayesian Computation. *Biometrika* 96(4), 983–990.
- Bierkens, J., P. Fearnhead, G. Roberts, et al. (2019). The Zig-Zag Process and Super-efficient Sampling for Bayesian Analysis of Big Data. *The Annals of Statistics* 47(3), 1288–1320.
- Blei, D. M., A. Kucukelbir, and J. D. McAuliffe (2017). Variational Inference: a Review for Statisticians. *Journal of the American Statistical Association* 112(518), 859–877.
- Boltz, S., E. Debreuve, and M. Barlaud (2009). High-dimensional Statistical Measure for Region-of-interest Tracking. *IEEE Transactions on Image Processing* 18(6), 1266–1283.
- Carvalho, C. M., N. G. Polson, and J. G. Scott (2010). The Horseshoe Estimator for Sparse Signals. *Biometrika* 97(2), 465–480.
- Deheuvels, P. et al. (1986). On the Influence of the Extremes of an IID Sequence on the Maximal Spacings. *The Annals of Probability* 14(1), 194–208.
- Devroye, L. et al. (1982). A Log Log Law for Maximal Uniform Spacings. *The Annals of Probability* 10(3), 863–868.
- Dinh, L., J. Sohl-Dickstein, and S. Bengio (2017). Density Estimation using Real NVP. In *International Conference on Learning Representations*.
- Dunson, D. B., N. Pillai, and J.-H. Park (2007). Bayesian Density Regression. *Journal of the Royal Statistical Society: Series B (Statistical Methodology)* 69(2), 163–183.
- El Moselhy, T. A. and Y. M. Marzouk (2012). Bayesian Inference with Optimal Maps. *Journal of Computational Physics* 231(23), 7815–7850.
- Fearnhead, P., J. Bierkens, M. Pollock, and G. O. Roberts (2018). Piecewise Deterministic Markov Processes for Continuous-time Monte Carlo. *Statistical Science* 33(3), 386–412.
- Giordano, R., T. Broderick, and M. I. Jordan (2018). Covariances, Robustness and Variational Bayes. *The Journal of Machine Learning Research* 19(1), 1981–2029.
- Janson, S. (1987). Maximal Spacings in Several Dimensions. *The Annals of Probability* 15(1), 274–280.
- Levy, D., M. D. Hoffman, and J. Sohl-Dickstein (2018). Generalizing Hamiltonian Monte Carlo with Neural Networks. In *International Conference on Learning Representations*.
- Neal, R. M. et al. (2011). MCMC using Hamiltonian Dynamics. *Handbook of markov chain monte carlo* 2(11), 2.
- Parno, M. D. and Y. M. Marzouk (2018). Transport Map Accelerated Markov Chain Monte Carlo. *SIAM/ASA Journal on Uncertainty Quantification* 6(2), 645–682.
- Paszke, A., S. Gross, S. Chintala, and G. Chanan (2017). PyTorch: Tensors and Dynamic Neural Networks in Python with Strong GPU Acceleration. *PyTorch: Tensors and dynamic neural networks in Python with strong GPU acceleration* 6.
- Piironen, J. and A. Vehtari (2017). Sparsity Information and Regularization in the Horseshoe and Other Shrinkage Priors. *Electronic Journal of Statistics* 11(2), 5018–5051.
- Robert, C. P., V. Elvira, N. Tawn, and C. Wu (2018). Accelerating MCMC algorithms. *Wiley Interdisciplinary Reviews: Computational Statistics* 10(5), e1435.
- Roberts, G. O., R. L. Tweedie, et al. (1996). Exponential Convergence of Langevin Distributions and Their Discrete Approximations. *Bernoulli* 2(4), 341–363.
- Santambrogio, F. (2015). Optimal Transport for Applied Mathematicians. *Birkäuser, NY* 55, 58–63.

Appendix

Proof of theorem 1

Proof. It is trivial to see that (2) holds. For (3), we show its existence via one (among many) construction. For any measurable \mathcal{A} , denote the conditional probability

$$\int_{\mathcal{A}} \frac{P(\theta, \beta)}{\Pi(\theta | Y)} d\beta = \mu(\mathcal{A}) \in (0, 1].$$

As any measurable function is the pointwise limit of simple function, for any $h : \Theta \rightarrow \mathbb{R}$ measurable, there exists limit

$$h(\beta) = \lim_{n \rightarrow \infty} \sum_{i=1}^n g_{[n]i} 1(\beta \in E_{[n]i}),$$

where $E_{[n]1}, \dots, E_{[n]n}$ the disjoint partition of Θ and $g_{[n]i}$ a constant depending on $E_{[n]i}$.

Integrate over β ,

$$\int h(\beta) d\beta = \lim_{n \rightarrow \infty} \sum_{i=1}^n g_{[n]i} \mu(E_{[n]i}).$$

As $\mathcal{A} \neq \emptyset$, we can choose $E_{[n]i}$ small enough such that $\mathcal{A} = \cup_{i \in I} E_{[n]i}$ with I some set of i . Therefore $\mathcal{A} \cap E_{[n]i} = \emptyset$ unless $E_{[n]i} \subseteq \mathcal{A}$. Take $h(\beta)$ to be $1(\beta \in \mathcal{A})$, the left hand side is $\mu(\mathcal{A})$, choose the right hand side $g_{[n]i} = 1(E_{[n]i} \subseteq \mathcal{A})$.

Given β , the integral using (4) has

$$\int_{\mathcal{A}} P(\beta | \theta) d\beta = \sum_{k=1}^{\infty} w_k(\theta) 1\{f_k^{-1}(\theta) \in \mathcal{A}\}.$$

For each k , let $w_k(\theta) = \mu(E_{[n]i})$ and f_k satisfy $f_k^{-1}(\Theta) \subseteq E_{[n]i}$, so that $1\{f_k^{-1}(\theta) \in \mathcal{A}\} = g_{[n]i}$, this yields the result. \square

Proof of theorem 2

Proof.

$$\begin{aligned} \Pi_r(\beta) &= \int \sum_{k=1}^K w_k(\theta) \Pi(\theta | Y) \delta\{\beta - f_k^{-1}(\theta)\} d\theta \\ &= \sum_{k=1}^K \int w_k(\theta) \Pi(\theta | Y) \delta\{\theta - f_k(\beta)\} |\det \nabla f_k(\beta)| d\theta \\ &= \sum_{k=1}^K w_k\{f_k(\beta)\} \Pi\{f_k(\beta) | Y\} |\det \nabla f_k(\beta)|, \end{aligned}$$

where the Jacobian emerges due to $\delta\{g(x)\} = \delta(x - x_0) |\det \nabla g(x_0)|^{-1} = \delta(x - x_0) |\det \nabla g^{-1}(x_0)|$ with $g(x_0) = 0$ for invertible g . \square

Proof of theorem 3

Proof. The task is equivalent to showing $\log\{g(\beta)\}$ has a bounded derivative almost everywhere. Rewriting

$$\begin{aligned}\log\{g(\beta)\} &= \log \sum_{k=1}^K \exp h_k(\beta), \\ h_k(\beta) &= -\log K + \log \Pi_r(\beta) - \log w_k\{f_k(\beta)\} - \log L\{Y \mid f_k(\beta)\} \Pi_0\{f_k(\beta)\} - \log |\det \nabla f_k(\beta)|\end{aligned}$$

and taking derivative with respect to the m th sub-coordinate of β , denoted by $\beta_{[m]}$, its magnitude satisfies

$$\begin{aligned}\left| \frac{\partial \log\{g(\beta)\}}{\partial \beta_{[m]}} \right| &= \left| \sum_{k=1}^K \frac{\exp h_k(\beta) \partial h_k(\beta) / \partial \beta_{[m]}}{\sum_{l=1}^K \exp h_l(\beta)} \right| \\ &\leq \sum_{k=1}^K \frac{\exp h_k(\beta)}{\sum_{l=1}^K \exp h_l(\beta)} \left| \frac{\partial h_k(\beta)}{\partial \beta_{[m]}} \right| \\ &\leq \max_{k \in \{1 \dots K\}} \left| \frac{\partial h_k(\beta)}{\partial \beta_{[m]}} \right|.\end{aligned}$$

Examining the derivative yields

$$\left| \frac{\partial h_k(\beta)}{\partial \beta_{[m]}} \right| \leq \left| \frac{\partial \log \Pi_r(\beta)}{\partial \beta_{[m]}} \right| + \left| \frac{\partial \log w_k(\theta) L\{Y \mid \theta\} \Pi_0(\theta)}{\partial \theta} \Big|_{\theta=f_k(\beta)} \right| \left| \frac{\partial f_k(\beta)}{\partial \beta_{[m]}} \right| + \sum_{\text{all } s^k} \left| \frac{\partial \log |s^k|}{\partial \beta_{[m]}} \right|.$$

By absolute continuity, the first two absolute values are finite almost everywhere. For the third term, $|\partial f_k(\beta) / \partial \beta_{[m]}| = \prod_{\text{all } s^k} |s^k| < \infty$. For the last term, each s^k is a finite composition of Lipschitz functions, therefore it is Lipschitz with respect to β ; as $s^k > 0$, each derivative is equal to $\partial |s^k| / \partial \beta_{[m]} / |s^k| < \infty$.

Denote the index that achieves the minimum distance as $i_0 = \arg \inf_{i \in \{1 \dots n\}} \|\beta^* - \beta_i\|$, then

$$\inf_{i \in \{1 \dots n\}} \|\log\{g(\beta^*)\} - \log\{g(\beta_i)\}\| \leq \|\log\{g(\beta^*)\} - \log\{g(\beta_{i_0})\}\| = \mathcal{O}(\|\beta^* - \beta_{i_0}\|).$$

Combining the above yields the result. □